J. Biomed. Eng. Res.
Vol.26, No.1, 17-22, 2005

Development of Analytical Model for Optimization of Dual Layer Phoswich Detector Length for PET

Yong Hyun Chung, Yong Choi, Yearn Seong Choe, Kyung-Han Lee, Byung-Tae Kim

Department of Nuclear Medicine, Samsung Medical Center, Samsung Biomedical Research Institute
Sungkyunkwan University School of Medicine
(Received October 5, 2004. Accepted November 25, 2004)

Abstract: Small animal PET using a dual layer phoswich detector has been developed to obtain high and uniform spatial resolution. In this study, a simple analytic model to optimize the lengths of a dual layer phoswich detector was derived and validated by Monte Carlo simulation. For a small animal PET scanner with a 10 cm ring diameter, the optimal length of the phoswich detector consisting of various crystal materials, such as LSO and LuYAP, were calculated analytically and validated using GATE. The detector module consisted of 8 × 8 arrays of crystals, with each phoswich detector element having a 2 mm × 2 mm sensitive area. The total crystal length was fixed to 20 mm. The optimal lengths of the phoswich detector layers, as functions of the crystal materials and order, conveniently derived by the analytic equation, showed good agreement with those estimated by the time consuming simulation. The simple analytical model can be used for the fast and accurate design of an optimal phoswich detector for small animal PET to achieve high spatial resolution and uniformity.

Key words: Small animal PET, Depth of interaction, Parallax error, Dual layer phoswich detector

INTRODUCTION

Small animal PET should have high sensitivity, greater than 2%, and uniform resolution across the field of view (FOV), in the order of 2 mm, to achieve an image quality for rodents comparable to that of humans [1-4]. In order to increase the sensitivity and resolution and to reduce the number of detector modules (and hence cost) of small animal PET, a long narrow crystal pixel array and small ring diameter were used. However, they lead to spatial resolution degradation, known as radial elongation or parallax error. The annihilation events originating off-center of the FOV might register to an inaccurate line of response (LOR) and degrade the image resolution, as most are obliquely incident on the crystal surface, penetrate into the adjacent several crystal pixels before interacting, and are presented only by information of the interacting crystal.

This study was supported by National Nuclear Technology Program, Ministry of Science & Technology and by a grant of the Korea Health 21 R&D Project (02-PJ3-PG6-EV06-0002), Ministry of Health & Welfare, Republic of Korea.
Corresponding Author: Yong Choi, Samsung Medical Center, Sungkyunkwan University, 50 Ilwon-dong, Kangnam-gu, Seoul, Korea
Tel. (02) 3410-2624, Fax. (02) 3410-2639
E-mail. ychoi@skku.edu

This spatial resolution degradation increases for objects placed further away from the center of the FOV, and can be reduced significantly by determining the depth of interaction (DOI) in the crystal and by taking into account the DOI information when sorting coincident events [5-14].

With such information, the event can be assigned to the LOR that connects the interaction points rather than the interacting crystals, and as the LOR will pass through the source, parallax errors can be corrected.

The development of a detector module capable of accurately measuring the DOI is an active field of research, and a number of DOI determination schemes have been proposed. These include the use of a phoswich detector consisting of two or more layers of scintillation crystals that possess different decay times or light yields [11-13], coupling the photosensitive detectors to opposite ends of the crystal in order to measure the ratio of the two detector signals [6, 14], and a multistage rectangular block of crystals segmented along the depth, which use the light distribution property of the crystals [10]. Among the DOI identification schemes, the dual layer phoswich detector has been widely investigated by many research groups, and implemented in commercially available small animal PET [15] and human brain tomograph [16] due to its practicability and effectiveness at extracting DOI information. For small animal PET, the effects of the dual layer phoswich

detector on correcting parallax error were characterized, and lengths and order of each layer were optimized using Monte Carlo simulation [17]. However, in order to evaluate the radial elongation as functions of the length and order of the phoswich detector, a time consuming simulation is required, as the radial resolution of the simulated images should be measured for each source location, along with the radial axis, and for each combination of the phoswich detector order and lengths.

In this study, a simple analytical form for the calculation of the optimal lengths of the phoswich detector was derived. This method can estimate the effect of the DOI on the broadening of the spatial resolution for a ring-type PET consisting of dual-layer phoswich detector arrays. For various combinations of front and back layer materials of the phoswich detector, the optimal lengths of the front layer of the proposed scanners were calculated using the analytical model derived in this study, and compared to those estimated by Monte Carlo simulation.

MATERIALS AND METHODS

Analytical Model

Simple models of a small animal PET scanner and detector module are illustrated in Figure 1. The ring-type PET scanner, consisting of detector modules with a radius R, was modeled. Each detector module consisted of $N \times N$ pixels of two-layer scintillation crystals, each of which had the width l_p, the front layer length l_f, the back layer length l_b and the total length l_t.

The angle between a detector surface and an obliquely incident photon can be expressed by:

$$\sin(\theta) = \frac{P}{R} \tag{1}$$

where P is the distance between the scanner center and the position of the detected annihilation event and θ is the entrance angle of gamma rays onto the detector module.

It was assumed that the crystal in which a scintillation event occurs can be correctly identified, thus producing two DOI levels. The event occurring in the crystal layer can be represented by the number of penetrated front or back layers.

$$\text{If } \theta \geq a\tan\left(\frac{N \times l_p}{l_t}\right),$$

$$n = ceil\left(\frac{l_f \times \tan\theta}{l_p}\right),$$

$$m = ceil\left(\frac{N \times l_p - l_f \times \tan\theta}{l_p}\right) \tag{2}$$

else,

$$n = ceil\left(\frac{l_f \times \tan\theta}{l_p}\right),$$

$$m = ceil\left(\frac{l_b \times \tan\theta}{l_p}\right) \tag{3}$$

where n is the number of penetrated front layers, m is the number of penetrated back layers and the *ceil(x)* function rounds x upwards to the nearest integer.

The LOR for a pair of crystal layers is the line connecting the midpoints of their front faces. The tangent distance between the trajectory of the incident gamma ray (true LOR) and the calculated LOR is given by:

$$LOR_{f,n} = \left(n - \frac{1}{2}\right) \times l_p \times \cos\theta \tag{4}$$

$$LOR_{b,m} = \left\{\left(n + m - \frac{3}{2}\right) \times l_p - l_f \times \tan\theta\right\} \times \cos\theta \tag{5}$$

where $LOR_{f,n}$ is the tangent distance between the true and the calculated LORs connecting the n_{th} front layer, and $LOR_{b,m}$ is for the calculated LOR connecting the m_{th} back layer, as shown in Figure 2.

The probabilities of the photon interaction in the n_{th} front layer, F_n or the m_{th} back layer, B_m are given by:

$$F_n = (1 - F_{n-1}) \times (1 - e^{-\mu_f \times \frac{l_p}{\sin\theta}}) \tag{6}$$

$$B_m = (1 - F_n - B_{m-1}) \times (1 - e^{-\mu_b \times \frac{l_p}{\sin\theta}}) \tag{7}$$

where μ_f and μ_b are the attenuation coefficients of the front and back layer crystals, respectively.

F_n and B_m can be represented as a function of the distance between the true and calculated LORs, which were characterized from two linear lines using multiple linear regression curve fitting, as shown in Figure 3. Figure 3 shows the probabilities of photon interaction for the phoswich detector consisting of LSO and LuYAP, popular scintillation materials due to their high densities and light yield with current PET. The x-coordinate at the point of intersection of two lines was defined as a reference value, V_{ref}, for the spatial resolution broadening. It was assumed that the spatial broadening was mainly affected by events

having longer $LOR_{f,n}$ or $LOR_{b,m}$ than the reference value. For all values of n and m satisfying $LOR_{f,n} > V_{ref}$ and $LOR_{b,m} > V_{ref}$, the $factor_{DOI}$ was defined as follows:

$$factor_{DOI} = \sum_{n} F_n + \sum_{m} B_m \qquad (8)$$

By minimizing the $factor_{DOI}$, the degradation of the spatial resolution can be minimized.

For a small animal PET scanner with a 10 cm ring diameter, the optimal lengths of the phoswich detector consisting of various crystal materials, such as LSO and LuYAP, were calculated using this analytical model. The detector module consisted of 8 × 8 arrays of crystals, with each phoswich detector element having a 2 mm × 2 mm sensitive area. The total crystal length was fixed to 20 mm.

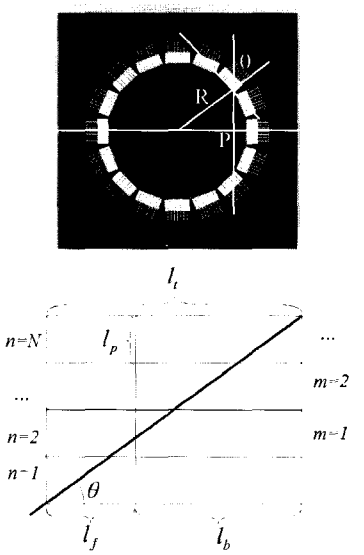

Fig. 1. Simple model of a small animal PET scanner (top) and detector module (bottom).

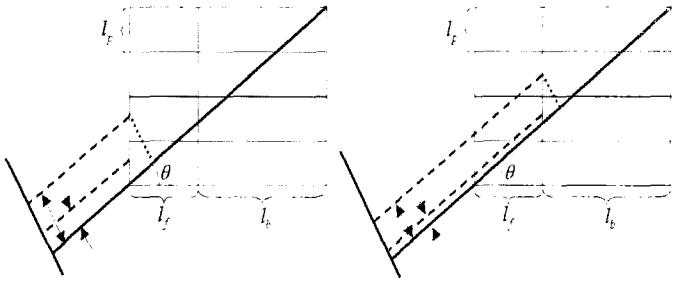

Fig. 2. The tangent distances (arrows) between the incident line of the gamma ray (straight line) and calculated LOR (dashed line) connecting the n_{th} front layer (left) or the m_{th} back layer (right).

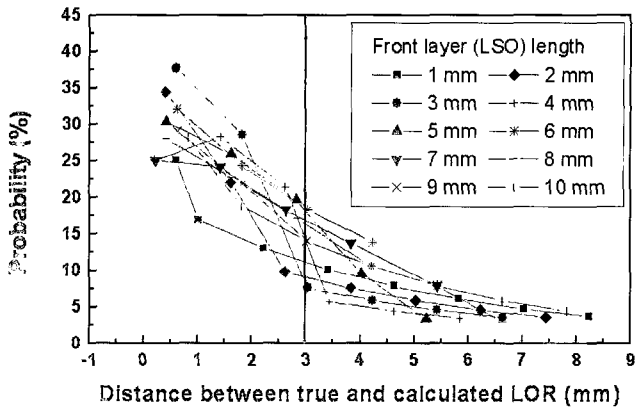

Fig. 3. Probability of gamma ray interaction as a function of the distance between true and calculated LORs for an LSO-LuYAP phoswich detector.

Validation of Analytic Model with Monte Carlo Simulation

In order to validate the analytical model, which estimated the effects of dual layer phoswich detector on the PET image qualities as functions of the order and lengths of the crystals, Monte Carlo simulation, using GATE (GEANT4 Application for Tomographic Emission), was performed.

GATE is a new Monte Carlo simulation platform based on the well-proven simulation tool, GEANT4 [18], which was developed to model various phenomena encountered in SPECT and PET applications using a scripting language [19-23]. The complex geometry of ring-type PET detectors, phantoms, and any number of radioactive sources with different properties, can be easily simulated with GATE. Each gamma photon is tracked until its energy falls below the energy threshold or it escaped from the system, where the physical process of the gamma interaction, with the exception of the light transportation, is modeled. A detected position, deposited energy and time information for each single event are stored. The coincidence event, occurring between only two layers, are sorted with various time windows, and the spatial coordinates of the barycenters of coincident layers are extracted to make a sinogram with the DOI information. Images are reconstructed using 2D filtered back projection, with a Ramp filter.

A small animal PET with a 10 cm ring diameter was designed for simulation. The simulated PET employed 16 dual-layer phoswich detector modules, consisting of LSO and LuYAP crystals. The detector module consisted of 8 × 8 arrays of phoswich crystals, with each phoswich element having a 2 mm × 2 mm sensitive area and a 2.3 mm pitch. The total phoswich crystal length was fixed at 20 mm, and the order and lengths of the front and back crystal layers altered to examine their effects on the DOI

measurement. For each front and back layer combination of the phoswich detector, the radial resolution of the proposed scanner was estimated. A 0.1 mm diameter Na-22 point source was positioned 40 mm off-center of the scanner FOV along the central axis in 10 mm steps. After images of the source at each position had been reconstructed, the FWHMs of the radial profiles were estimated by Gaussian fitting.

RESULTS

The $factor_{DOI}$ of the 10 cm diameter ring scanners, as a function of the front layer length, were calculated for various combinations of dual layer phoswich crystals. Figure 4 shows the $factor_{DOI}$ for the LSO-LuYAP phoswich detector as a function of the front layer length. When the front layers of the phoswich detector were 5 mm long for LSO and 6 mm long for LuYAP, the minimal $factor_{DOI}$ was achieved for the expected uniform radial resolution of the small PET. Optimal lengths of the front layer for various phoswich detector configurations are listed in Table 1.

Table 1. Optimal lengths of the front layers, as estimated by the analytical model and GATE simulation for various dual layer phoswich detector configurations.

Front layer	Back layer	Optimal length of front layer (Analytic Model / GATE)
LSO	LuYAP	5 mm / 5 mm
LuYAP	LSO	6 mm / 6 mm

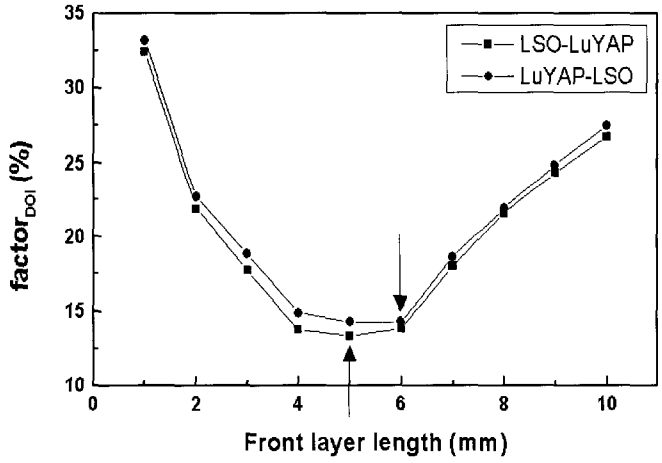

Fig. 4. $factor_{DOI}$ as a function of the front layer length for an LSO-LuYAP phoswich detector.

The simulated radial resolutions for the LSO-LuYAP phoswich detector as a function of the front layer length are demonstrated in Figure 5. These figures demonstrate the improved spatial resolution when the DOI information was measured using the phoswich detector. As illustrated in Figures 5, the radial resolutions at 40 mm off-center were 5.6, 3.4, 4.1 and 7.9 mm with LSO front layer lengths of 2, 5, 10 and 20 mm, respectively. For the LuYAP front layer phoswich detector, the radial resolutions at 40 mm off-center were 6.2, 3.7, 4.0, and 8.0 mm with front layer lengths of 2, 6, 10 and 20 mm, respectively. The best uniformity in the radial distribution of the spatial resolution was achieved when the front layer lengths were 5 mm and 6 mm for LSO and LuYAP front layer phoswich detectors, respectively.

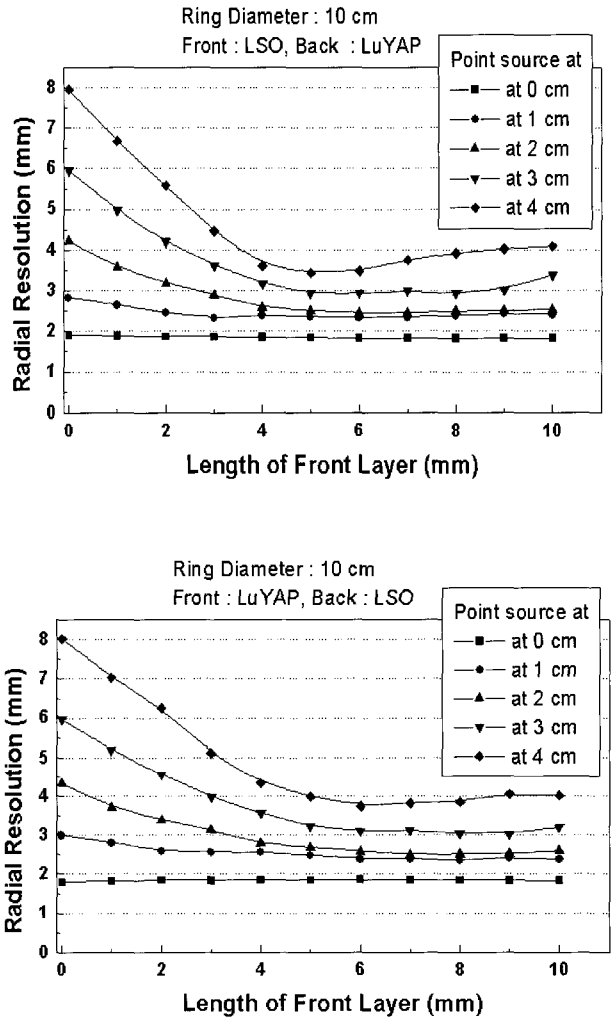

Fig. 5. Simulated radial resolution as a function of the front layer length for a 10 cm diameter scanner with an LSO front layer phoswich detector (top) and a LuYAP front layer phoswich detector (bottom).

DISCUSSION AND CONCLUSION

An analytical model for estimating the optimal length of each layer of a dual layer phoswich detector, by calculating the penetration probability of the photon most obliquely incident on the detector module, was derived. The effects of the crystal layer order and lengths of the phoswich detector on the DOI measurements and image qualities were characterized and optimized as a function of the front layer length of the phoswich detector using both the analytical model and Monte Carlo simulation. The optimal lengths of the front layer for phoswich detectors consisting of LSO and LuYAP crystal materials estimated with this model agreed well with those of the time-consuming GATE simulation.

The results obtained in this study demonstrate that the difference in the ratio between the calculated and true LORs and the radial resolution degradation was considerably improved by the DOI information. It was found that the optimal crystal layer lengths of the phoswich detector are altered by the material type and layer order, since the photon penetrations of crystals are dependent on their absorption properties.

The simple analytical model derived in this study can efficiently estimate the lengths of the phoswich detector, which minimizes the DOI-induced resolution degradation, as a function of the crystal material type, order and total length. If a Monte Carlo simulation is used to obtain the information, although the spatial resolution of scanner can be directly estimated, extensive calculations are required which could take more than twenty hours. Therefore, this model can be used for the fast and accurate design of an optimal phoswich detector for small animal PET for achieving high and uniform spatial resolution.

REFERENCES

[1] Y. H. Chung, T. Y. Song, and Y. Choi, "*Nuclear medicine imaging instrumentations for molecular imaging*", Korean Journal of Nuclear Medicine, Vol. 38, No. 2, pp. 131-139, 2004.

[2] R. S. Balaban, and V. A. Hampshire, "*Challenges in small animal noninvasive imaging*", ILAR Journal, Vol. 42, pp. 248-262, 2001.

[3] R. Myers, and S. Hume, "*Small animal PET*", European Neuropsychopharmacology, Vol. 12, pp.545-555, 2002.

[4] A. F. Chatziioannou, S. R. Cherry, Y. Shao, R. W. Silverman, K. Meadors, T. H. Farquhar, M. Pedarsani, and M.E. Phelps, "*Performance evaluation of microPET: a high-resolution Lutetium oxyorthosilicate PET scanner for animal imaging*", Journal of Nuclear Medicine, pp. 1164-1175, 1999.

[5] P. Bartzakos, and C. L. Thompson, "*A depth-encoded PET detector*", IEEE transactions of Nuclear Science, Vol. 38, pp. 732-738, 1991.

[6] W. W. Moses, S. E. Derenzo, C. L. Melcher, and R. A. Manente, "*A room temperature LSO/PIN photodiode PET detector module that measures depth of interaction*", IEEE transactions of Nuclear Science, Vol. 42, pp. 1085-1089, 1995.

[7] C. Moisan, G. Tsang, J. G. Rogers, and E. M. Hoskinson, "*Performance studies of a depth encoding multicrystal detector for PET*", IEEE transactions of Nuclear Science, Vol. 43, pp. 1926-1931, 1996.

[8] L. R. MacDonald, and M. Dahlbom, "*Depth of interaction for PET using segmented crystals*", IEEE transactions of Nuclear Science, Vol. 45, pp. 2144-2148, 1998.

[9] R. S. Miyaoka, T. K. Lewellen, H. Yu, and D. L. MacDaniel, "*Design of a depth of interaction (DOI) PET detector module*", IEEE transactions of Nuclear Science, Vol. 45, pp. 1069-1073, 1998.

[10] H. Murayama, H. Ishibashi, H. Uchida, T. Omura, and T. Yamashita, "*Depth encoding multicrystal detectors for PET*", IEEE transactions of Nuclear Science, Vol. 45, pp. 1152-1157, 1998.

[11] S. Yamamoto, and H. Ishibashi, "*A GSO depth of interaction detector for PET*", IEEE transactions of Nuclear Science, Vol. 45, pp. 1078-1082, 1998.

[12] J. Seidel, J. J. Vaquero, S. Siegel, W. R. Gandler, and M. V. Green, "*Depth Identification accuracy of a three layer phoswich PET detector module*", IEEE transactions of Nuclear Science, Vol. 46, pp. 485-490, 1999.

[13] U. Heinrichs, U. Pietrzyk, and K. Ziomons, "*Design optimization of the PMT-ClearPET prototypes based on simulation studies with GEANT3*", IEEE transactions of Nuclear Science, Vol. 50, pp. 1428-1432, 2003.

[14] Y. Shao, R. W. Silverman, R. Farrell, L. Cirignano, R. Grazioso, K. S. Shah, G. Vissel, M. Clajus, T. O. Tumer, and S. R. Cherry, "*Design studies of a high resolution PET detector using APD arrays*", IEEE transactions of Nuclear Science, Vol. 47, pp. 1051-1057, 2000.

[15] J. Seidel, J. J. Vaquero, and M. V. Green, "*Resolution uniformity and sensitivity of the NIH ATLAS small animal PET scanner: comparison to simulated LSO scanner without depth-of-interaction capability*", IEEE transactions of Nuclear Science, Vol. 50, pp. 1347-1350, 2003.

[16] K. Wienhard, M. Schmand, M. E. Casey, K. Baker, J. Bao, L. Eriksson, W. F. Jones, C. Knoess, M. Lenox, M. Lercher, P. Luk, C. Michel, J. H. Reed, N. Richerzhagen, J. Treffert, S. Vollmar, J. W. Young, W. D. Heiss, and R. Nutt, "*The ECAT HRRT: Performance and first clinical application of the new high resolution research tomography*", IEEE transactions of Nuclear Science, Vol. 49, pp. 104-110, 2002.

[17] Y. H. Chung, Y. Choi, G. Cho, Y. S. Choe, K-H. Lee, B-T. Kim, "*Characterization of Dual Layer Phoswich Detector Performances for Small Animal PET using Monte Carlo Simulation*", Physics in Medicine and Biology, Vol. 49, No. 13, pp. 2881-2890, 2004.

[18] GEANT4 Collaboration, GEANT4: A simulation toolkit, SLAC Report SLAC-PUB-9350, 2002.

[19] S. Jan, G. Santin, D. Strul, S. Staelens, K. Assie, D. Autret, S. Avner, R. Barbier, M. Bardies, P. M. Bloomfield, D. Brasse, V. Breton, P. Bruyndonckx, I. Buvat, A. F. Chatziioannou, Y. Choi, Y. H. Chung, C. Comtat, D. Donnarieix, L. Ferrer, S. J. Glick, C. J. Groiselle, D. Guez, P. F. Honore, S. Kerhoas-Cavata, A. S. Kirov, V. Kohli, M. Koole, M. Krieguer, D. J. van der Laan, F. Lamare, G. Largeron, C. Lartizien, D. Lazaro, M. C. Maas, L. Maigne, F. Mayet, F. Melot, C. Merheb, E. Pennacchio, J. Perez, U. Pietrzyk, F. R. Rannou, M. Rey, D. R. Schaart, C. R. Schmidtlein, L. Simon, T. Y. Song, J. M. Vieira, D. Visvikis, R. Van de Walle, E. Wieers, and C. Morel, "*GATE: a simulation toolkit for PET and SPECT*", Physics in Medicine and Biology, Vol. 49, No. 19, pp. 4543-4561, 2004.

[20] S. Staelens, D. Strul, G. Santin, S. Vandenberghe, M.

Koole, Y. D'Asseler, I. Lemahieu, and R. V. Walle, *"Monte Carlo simulations of a scintillation camera using GATE: validation and application modeling"*, Physics in Medicine and Biology, Vol. 48, pp. 3021-3042, 2003.

[21] G. Santin, D. Strul, D. Lazaro, L. Simon, M. Krieguer, M. V. Martins, V. Breton, and C. Morel, *"GATE: A Geant4-based simulation platform for PET and SPECT integrating movement and time management"*, IEEE transactions of Nuclear Science, Vol. 50, pp. 1516-1521, 2003.

[22] D. Lazaro, I. Buvat, G. Loudos, D. Strul, G. Santin, N. Giokaris, D. Donnarieix, L. Maigne, V. Spanoudaki, S. Styliaris, S. Staelens, and V. Breton, *"Validation of the GATE Monte Carlo simulation platform for modelling a CsI(Tl) scintillation camera dedicated to small-animal imaging"*, Physics in Medicine and Biology, Vol. 49, pp. 271-285, 2004.

[23] J. H. Jung, Y. Choi, Y. H. Chung, T. Y. Song, M. H. Jeong, K. J. Hong, B. J. Min, Y. S. Choe, K-H. Lee, and B-T. Kim, *"A computer simulation for small animal Iodine-125 SPECT development"*, Korean Journal of Nuclear Medicine, Vol. 38, No.1, pp. 74-84, 2004.